

Hydrogenation of benzene in gasoline fuel over nanoparticles (Ni, Pt, Pd, Ru and Rh) supported fullerene: Comparison study

Hassan Keypour¹ and Mohammad Noroozi^{*,1,2}

¹Faculty of Chemistry, Bu-Ali Sina University, Hamedan 65174, Iran,

²Center for Research and Development of Petroleum Technologies at Kermanshah, Research Institute of Petroleum Industry (RIPI), Kermanshah, Iran

Article history:

Received: 6/Jun/2014

Received in revised form: 10/Jul/2014

Accepted: 25/Jul/2014

Abstract

The main purpose of the present study is to synthesis different fullerene (C₆₀)-based metal (Ni, Pd, Pt, Ru and Rh) nanocatalysts that is used for the catalytic hydrogenation of benzene in gasoline. Metal catalysts were then loaded with the impregnation method and deposited on the functionalized fullerene. Response surface methodology (RSM) was used to investigate the cumulative effect of various parameters including pressure, temperature, time and loading and to optimize these parameters to maximizing the hydrogenation of benzene in gasoline. The catalysts were characterized before reaction by XRD, TEM and TGA. The results show that the yield of hydrogenation under optimum conditions (include metal loading of about 10%, reaction time of 180 min and hydrogen pressure of 50 atm) are obtained: 99.59, 99.48, 98.09, 98.51 and 97.56%, for Rh, Ru, Pt, Pd and Ni, respectively. These results are obtained by the different reaction time for Rh, Ru, Pt, Pd and Ni following: 180, 125, 31.25, 180 and 180 min respectively.

Keywords: Hydrogenation, Nanocatalyst, Fullerene, Response Surface Methodolog

1. Introduction

Gasoline is a complex and highly variable volatile mixture which contains over 500 saturated and unsaturated hydrocarbons. Among these hydrocarbons, only 150 are detectable. The existing mixture of compounds in gasoline shows both temporal and geographic changes in its composition. In general, advanced gasoline contains approximately 14% aromatics, 80% paraffins, 6% olefins, and few amounts

of alcohol, ether, detergent, corrosion inhibitor, antioxidant, and oxygenate [1]. From a toxicological point of view, benzene is one of the most hazardous components because human exposure to this component can have carcinogenic effects. Several organizations including International Agency of Research on Cancer (IARC) [2] and the American Conference of Governmental Industrial Hygienists (ACGIH) have been demonstrated the dangerous effects of benzene [3].

*. **Corresponding Author:** E-mail address: norouzim@ripi.ir, mo.noroozi@gmail; Tel.: +(98) 83 38358077

The presence of benzene in the air is mainly due to the motor vehicle emissions. Therefore a few countries have recently passed some laws to reduce the levels of benzene in gasoline. Countries of the European Community such as USA, Japan, Brazil and others have been established 1% (v/v) limit as the maximum level of tolerance for benzene in automotive gasoline [4-9]. The reduction of benzene constituent in gasoline is becoming one of the most interesting research areas in the recent years. The Mobile Source Air Toxics (MSAT) rule that was published on February 26, 2007, requires that refiners and importers in the USA produce gasoline that has an annual average benzene content of 0.62 volume percent (vol %) or less, beginning in 2011 [10,11]. The catalysts of group VIII metals, such as Ni [12-26], Fe [27-29], Pt [30-32], Pd [33, 34], Ru [35-38] and Co [39-44], have been used for the hydrogenation of benzene. Among these catalysts, Ni and Pt-based catalysts have been extensively studied and are already used in commercial processes[45].

Catalysis has been envisaged as one of the various possible applications of fullerenes. This causes the pathways of researches to divide into different directions, which can be classified into three main groups: (i) the use of C₆₀ as a catalyst [46-47]; (ii) the use of C₆₀ as a ligand for homogeneous catalysts [48]; (iii) the use of fullerenes as a support medium for heterogeneous catalysts [49, 50]. Considerable amount of investigations have been made in relation to the application of these materials as catalysts or catalyst supports [51]. The catalytic properties of these solids are depending on the interaction between the carbon support and metal particles. Solid-state chemistry of fullerene-based materials has gain much interest, due to the novel electronic and structural properties of these compounds [52]. The purpose of the present study is to synthesis different fullerene (C₆₀)-based metal (Ni, Pd, Pt, Ru and Rh) nanocatalysts that is used for the catalytic hydrogenation of benzene in gasoline.

2. Experimental procedure

2.1. Materials and equipments

Fullerene (C₆₀) was purchased from Sigma-Aldrich Chemise GmbH Company (purity 99%). Other chemical materials including solvents and metal salts were purchased from both Merck and Aldrich and used without further purification. IR spectra were recorded using Shimadzu Fourier Transform Infrared spectra (FT-IR) 8400, FT-NMR Jeol 90 MHz, GC SRI8610C. Elemental analysis for C, H and N were performed using a Perkin-Elmer 2400 series analyzer. The X-ray powder diffractometer (XRD) was manufactured by Philips PW-1840 with monochromated Cu K_α radiation and λ 1.54 Å. SEM was measured using a Philips XL-30 (V=17kw,a=2.5μA). Thermogravimetric Analysis (TGA) was taken on a Mettler Toledo TGA SDTA 85-e instrument at 30-800°C with 10 °C/Min. The quantitative determination of active catalyst was carried out using a SHIMADZU AA-6100 Atomic Absorption Spectrometer (AAS) by dissolving samples in a mixture of HCl and HNO₃ at a ratio of 3 : 1 at 40 °C for 24 h. Determination of benzene in gasoline was carried out by gas chromatography (GC) model SRI.

2.2. Preparation of fullereneol

A reaction flask (50 ml) charged with 1.0 g fullerene and fuming sulfuric acid (15 ml) was stirred at 55– 60 °C under N₂ for 3 days to give a dark brown solution with orange suspensions. The resulting mixture was added dropwise into anhydrous diethyl ether (200 ml) with vigorous stirring in an ice bath to cause the precipitation of products. Precipitates were separated from solution by the centrifuge technique. They were then washed and centrifuged three times with anhydrous diethyl ether and twice with 2:1 anhydrous diethyl ether-acetonitrile and dried in vacuum at 40 °C to afford a brown-orange solid of polycyclosulfated fullerene derivative 2 (1.3 g). A reaction flask (100 ml) equipped with a condenser and an inert gas bubbler was charged with polycyclosulfated fullerene derivative (1.0 g) and distilled water (20 ml). The mixture was stirred at 85 °C under N₂ for 10 h to give a dark brown suspension. The suspended solid was separated from aqueous solution by centrifugation followed by washing twice with water and drying in vacuum at 40 °C to afford a brown solid

of polyhydroxylated fullerene derivative (fullerenol) [53].

2.3. Preparation of nanocatalysts

Fullerenol (0.5 g) were separately mixed with 10, 55 and 100 ml aqueous solutions of ((Ni(NO₃)₂ · 6H₂O (8.52 × 10⁻³M), PdCl₂ (4.70 × 10⁻³M), H₂PtCl₆ · 6H₂O (2.56 × 10⁻³M), RuCl₃ · 3H₂O (4.95 × 10⁻³M), RhCl₃ · 3H₂O (4.86 × 10⁻³M)), to obtain catalysts containing 1, 5.5 and 10% Ni/C₆₀, Pd/C₆₀, Pt/C₆₀, Ru/C₆₀, Rh/C₆₀, respectively. The obtained data are given in Table 1. Citric acid (3 gr) was added to the solutions to enhance the penetration and dispersion of metal ions into the catalysts [54]. In order to reach into the final volume (150 ml), the required amount of ethanol-water mixture (1:3 v/v) was added to the solution. The suspension was stirred vigorously at 50 °C for 6 h and sonicated for 30 min in ultrasonic bath (1.6MHz) to form a uniform suspension. The resulting suspension was cooled in a cold water bath, filtered and finally washed with ethanol and deionized water. The elemental analysis of the filtered solution revealed no trace of metal species, indicating the fact that all metals particles were adsorbed on the support. The resulting slurry was dried at 100 °C to remove the solvent, and then calcined in air at 550 °C for 4 h. The prepared samples were reduced under pure H₂ (400 mL/min) at 300 °C and atmospheric pressure for 3 h. Finally, the percentage of loaded metal in catalysts was measured by atomic absorption spectrophotometer. The results are presented in Table 1.

2.4. Catalysts characterization

Table 1. Dispersion values of the metal supported on fullerene (C₆₀)

Catalysts	Raw material for metal	Volume of metal salt solution (ml)	Metal loading (w/w %)		Loading efficiency (%)
			Calculated	Found ^a	
Ni-1	Ni(NO ₃) ₂ · 6H ₂ O	10	1	0.98	98.0
Ni-5	(8.52 × 10 ⁻³ M)	55	5.5	5.38	97.8
Ni-10		100	10	9.70	97.0
Pd-1	PdCl ₂	10	1	0.96	96.0
Pd-5	(4.70 × 10 ⁻³ M)	50	5.5	5.43	98.7
Pd-10		100	10	9.61	96.1
Pt-1	H ₂ PtCl ₆ · 6H ₂ O	10	1	0.95	95.0
Pt-5	(2.56 × 10 ⁻³ M)	50	5.5	5.34	97.0

The transition electron microscopy (TEM) images were taken on a Philips CM120 at an accelerating voltage of 120Kv. Thermogravimetric analysis (TGA) of the dried samples was performed on a METTLER TOLEDO TGA SDTA 851e in the temperature range 30-800°C and rate 10°C/min. X-ray powder diffraction (XRD) analysis was conducted by Philips instrument with graphite monochromatic Cu K α radiation ($\lambda = 1.5418 \text{ \AA}$) to confirm the formation of products. The quantitative determination of active catalyst was carried out by a SHIMADZU AA-6100 atomic absorption spectrometer through dissolving the samples in a mixture of HCl and HNO₃ at 3:1 ratio at 40°C for 24 h. Gas chromatography (GC) was carried out by SRI with a flame ionization detector (FID) and the following conditions: injector 250°C, FID, 250°C, column MXT - 624 (6% Cyanopropyl phenyl, 94% dimethyl polysiloxane, 30 meter, 0.53 mm ID) and column temperature program is: 55 to 215°C with rate 5°C/min, Carrier gas: helium, sample size: 0.1 μ L and total cycle time, 32 min.

2.5. Catalytic test

0.1 gr of the synthesized catalyst (M/C₆₀) was introduced into a 100 ml stainless steel autoclave reactor and reduced under the flow of H₂ at 300°C for 1 hr. Then 1 ml of produced gasoline in Kermanshah Refinery of Iran and 10 ml of n-hexane (as a solvent), were added to the reactor. Then the mixture was purified with N₂ for 10 min to remove the oxygen. The reaction was carried out in different pressures of hydrogen (1-50 bar), temperatures (25-250 °C) and

Pt-10		100	10	9.71	97.1
Ru-1	RuCl ₃ . 3H ₂ O	10	1	0.92	92.0
Ru-5	(4.95 × 10 ⁻³ M)	50	5.5	5.44	98.9
Ru-10		100	10	9.75	97.5
Rh-1	RhCl ₃ . 3H ₂ O	10	1	0.96	96.0
Rh-5	(4.86 × 10 ⁻³ M)	50	5.5	5.38	97.8
Rh-10		100	10	9.47	94.7

^a As determined by AAS for catalyst

times (30-180 min). Cyclohexane was the main product of the benzene hydrogenation. The yield of hydrogenation was determined by GC.

2.6. Efficiency of hydrogenation

Gas chromatography is one of the well-accepted techniques which is employed to quantify mixtures of organic compounds. The applied method in this work includes a capillary column that is equipped with a special temperature programmer and separates the gasoline components with high resolution. There was no trace of cyclohexane in the gasoline. By dividing the area under each peak of benzene (Ab) to the total area of peaks and multiplying the resulting number to 100, the content of benzene in gasoline will be equal to 5.6%. The hydrogenation efficiency can be calculated using two methods. At the first method, subsequent to the set-up process of GC system including column, injector, and detector temperature, the product of the hydrogenation reaction (1μL), was injected into the GC column. The only detected product of the benzene hydrogenation was cyclohexane. Moreover, the efficiency of the mentioned product can be obtained from the following Eq:

$$\% \text{ Efficiency} = \frac{Ac}{Ab} \times 100 \quad (1)$$

Table 2. Experimental range and levels of process variables and full factorial central composite design matrix of orthogonal and real values along with observed responses for the hydrogenation of benzene in gasoline with Ni

Run no.	Pressure (atm)	Temperature (°C)	Time (min)	Loading (%)	hydrogenation efficiency %		
					Found ^a	Predicted	Residual
1	1	1	-1	1	96	95.6	0.30
2	0	0	0	1	93	93.4	0.32
3	1	1	1	-1	71	71.4	-0.47
4	0	0	0	0	86	86.0	-0.45

Where 'Ac' is area under the cyclohexane peak, 'Ab' is area under the benzene peak in gasoline.

At the second method, product of hydrogenation reaction (1μL) was injected into the GC with the previous settings. Additionally, the reaction efficiency is calculated according to the formula (1), while in the current calculations, the area under the cyclohexane peak was replaced with the area under the benzene peak in the product. The obtained results were similar to the previous calculations and are shown in Table 2.

2.7. Central composite design analysis and optimization by response surface methodology involved in the hydrogenation of benzene

The effect of influential parameters including, initial pressure of hydrogen, reaction temperature, reaction time and the amount of loaded metal in catalysts on the hydrogenation of benzene to cyclohexane was studied by statistically designed experiments. These parameters were optimized by response surface methodology. An orthogonal full factorial central composite design with ($\alpha = 1$) and one replicate at the centre point, resulted in 31 experiments for each catalyst that covers the entire range of variables and can be used to optimize the key variables for the hydrogenation of benzene through a batch reactor. The design package Minitab 14 is a statistical program

5	-1	1	1	-1	68	65.5	-0.02
6	1	-1	1	1	97	96.5	2.40
7	-1	1	-1	1	95	93.3	0.43
8	-1	0	0	0	83	84.9	1.68
9	0	0	-1	0	85	85.5	-1.91
10	0	0	0	0	86	86.0	-0.58
11	-1	-1	-1	-1	64	62.4	-0.02
12	1	1	-1	-1	67	66.9	1.57
13	1	-1	-1	1	94	95.0	0.07
14	0	0	0	-1	63	63.4	-1.03
15	-1	1	1	1	93	94.3	-0.47
16	1	-1	1	-1	66	66.3	-1.34
17	0	0	0	0	86	86.0	-0.31
18	-1	1	-1	-1	62	63.5	-0.02
19	0	0	0	0	89	86.0	-1.56
20	0	0	0	0	86	86.0	2.97
21	0	0	0	0	86	86.0	-0.02
22	0	0	1	0	87	87.3	-0.02
23	-1	-1	1	1	95	93.7	-0.36
24	-1	-1	-1	1	94	94.6	1.29
25	1	1	1	1	99	99.2	-0.67
26	1	0	0	0	89	88.0	-0.20
27	0	1	0	0	87	87.9	0.97
28	0	0	0	0	86	86.0	-0.91
29	1	-1	-1	-1	64	63.7	-0.02
30	0	-1	0	0	86	86.0	0.21
31	-1	-1	1	-1	61	62.4	-0.02

Factors	Levels		
	-1	0	1
Pressure (atm)	1.0	25.5	50.0
Temperature (°C)	25.0	137.5	250.0
Time (min)	30	105	180
Loading (%)	1.0	5.5	10.0

^a As determined by GC

package that is using for the regression analysis of the obtained data and will estimate the coefficient of the regression equation. The equations were confirmed by ANOVA (analysis-of-variance) analysis, to determine the significance of each term in the equations fitted and to estimate the goodness of fit in each case. Operation conditions of the reaction varied as follows; hydrogen from 1 to 50 atm, temperature reaction from 25 to 250 °C, reaction time from 30 to 180 min and loaded metal in catalyst from 1 to 10 %. For example, the coded and actual values of four independent variables for Ru that

were obtained from response surface methodology are shown in Table 2.

3. Results and discussion

3.1. Thermogravimetric analysis

The thermal analysis data in inert atmosphere (N₂) are shown in Fig. 1. These curves are related to metal catalysts with 10% loading. Two main weight loss regions were observed in this figure for all the catalysts. The first weight loss occurred at a temperature range of 100 °C – 540 °C and was moderate. Another weight loss

was observed the temperature range of 660°C -750°C. A similar behaviour was observed for all catalysts. Resulted thermogram shows that solvent loss such as water and organic solvents in catalyst start at 100°C and carbon cage and amorphous carbon decompose start at 550°C [55]. The remaining weights percent up to the

temperature of 800 °C are equal to 80.81, 83.81, 84.82, 85.69 and 86.64 which are related to Pt, Pd, Ni, Ru and Rh, respectively. High levels of residual masses may be due to the presence of metal installed on the fullerene, perform TGA under nitrogen atmosphere and the calcined in air at 550 °C for 4 h.

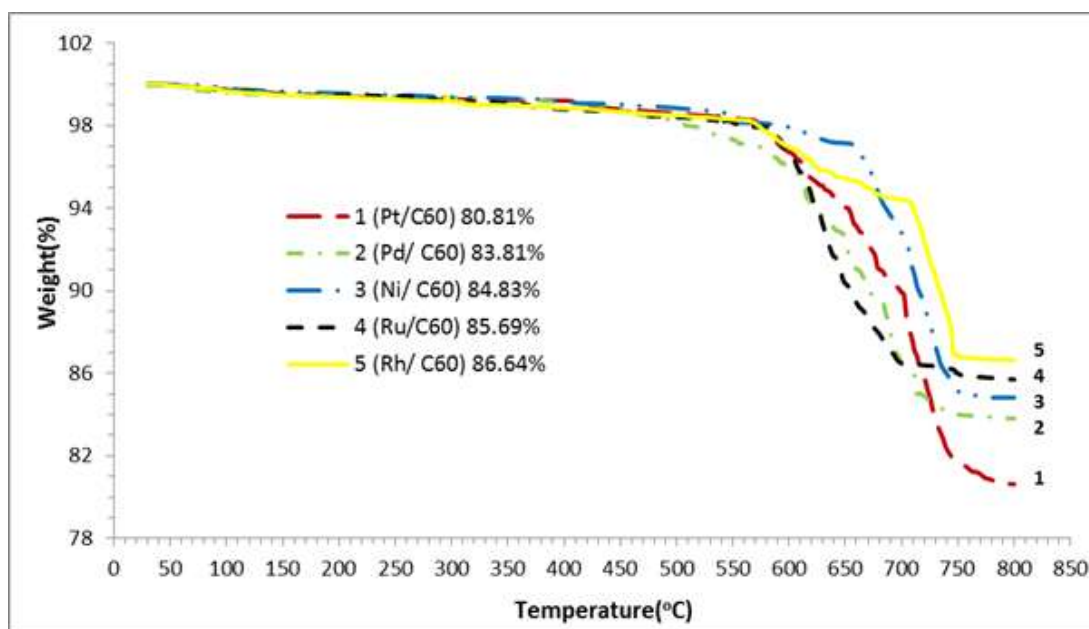


Fig 1. TGA profiles of selected catalysts

3.2. X-ray Diffraction analysis

The typical XRD patterns of Ni/C₆₀, Pd/C₆₀, Pt/C₆₀, Ru/C₆₀ and Rh/C₆₀ are presented in Fig. 2. The assignment of the various crystalline phases was based on the JPDS powder diffraction file cards [56]. The particle sizes of each phase were calculated from the line broadening of the most intense reflections using the Scherrer equation. Estimated errors of the particle sizes and relative percentage of different phases are on the order of 10% [57-60].

XRD patterns obtained for the Ni/C₆₀ show the presence of metallic nickel nanoparticles with almost no peaks corresponding to Ni-oxide. The peaks observed at a 2θ° of 44.5, 51.8 and 76.4° are characteristic of face centered cubic (fcc) nickel phase [61]. From the pattern, no characteristic peaks presenting hexagonal close-packed (hcp) nickel have been observed [62]. XRD pattern of Pd/C₆₀, as shown five reflection indexes of (100), (200), (220) and (311) were identified by the

cubic phase of Pd (card 05-0681 in the JCPDS file). The peak observed at 2θ°=40.98 indicating the fact that Pd is highly dispersed on the surface of fullerene with small crystalline size. The XRD pattern of platinum nanostructures (Fig 2) reveals that the obtained Pt nanocrystals possess cubic structure with high crystallinity. The four major peaks at a 2θ° of 39.8, 46.4, 67.7, and 81.8° can be assigned to the diffraction from the (111), (200), (220), and (311) planes of the fcc lattice of Pt (JCPDS Card No.04-0802), respectively. The structure of the Rh nanoparticle was determined to be (fcc) from the XRD pattern, as shown in Fig. 3. The five major peaks at a 2θ° of 39.8, 42.4, 50.7, 61 and 74.8° can be assigned to the diffraction from the (111), (200), (220), (311) and (222) planes. The XRD pattern obtained for the Ru/C₆₀ showed lower crystallinity. The peaks at a 2θ° 38.6, 42.3, 44 and 58.3 which agree well with the known diffraction pattern of ruthenium (JCPDS 6-663). The obtained clusters size of metal

nanoparticles Ni, Pd, Pt, Ru and Rh using the Scherrer formula are 18, 7.1, 25, 20.3 and 24 nm, respectively.

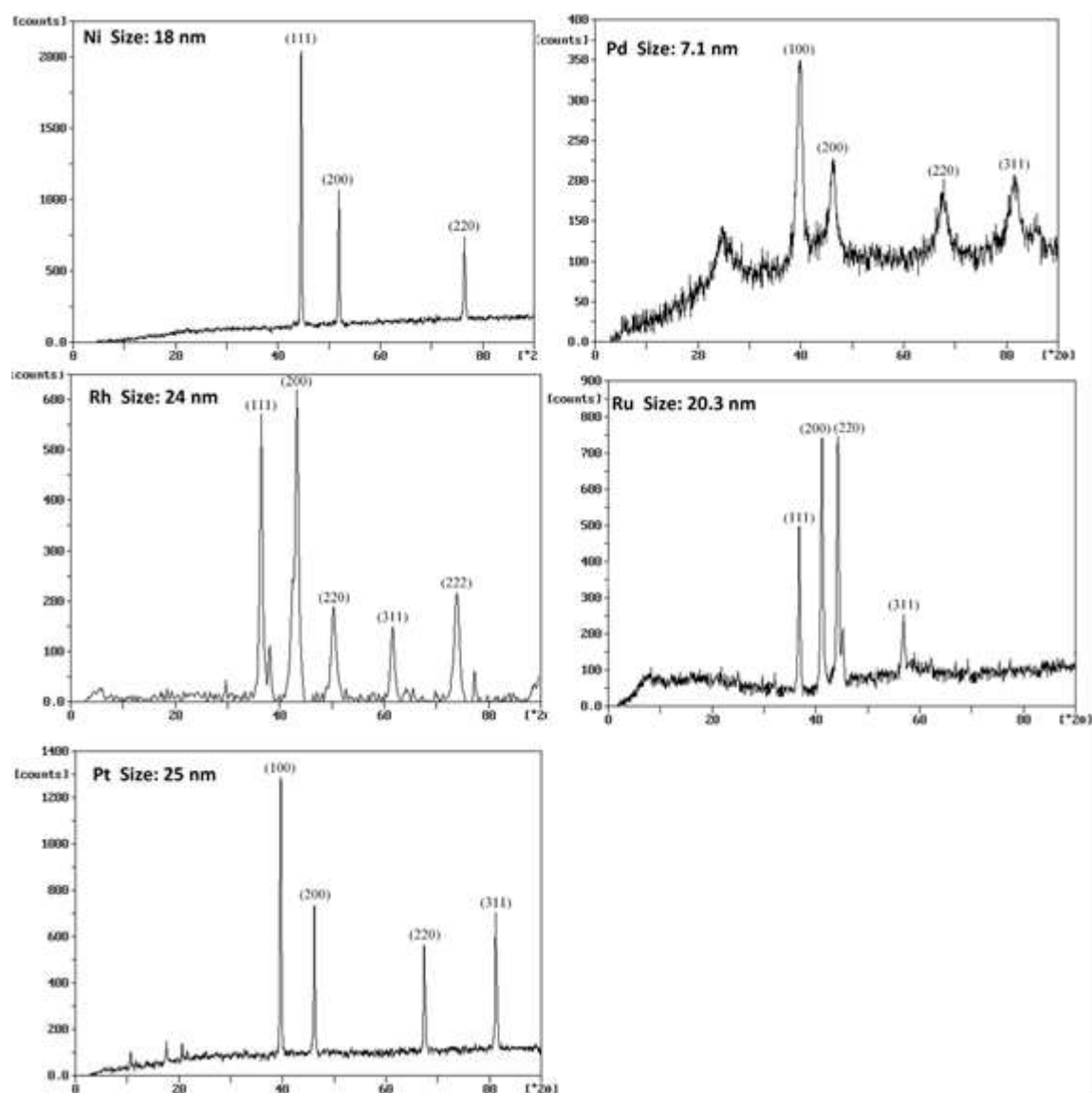


Fig. 2. XRD patterns of nano catalysts M/C₆₀ (M= Ni, Pd, Pt, Ru and Rh)

3.3 Transmission electron microscopy (TEM)

The average metal particle size of each catalyst was estimated by TEM. Average metal particle sizes of Ni, Pd, Pt, Ru and Rh are 12.3, 5.4, 21.3, 15.7 and 16.8 nm, respectively. The determined metal particle size by

TEM was compatible with the XRD data. Fig. 3 shows different images of TEM for catalysts. As seen in this figure, most of the metal particles are located on the external surface of the fullerenes.

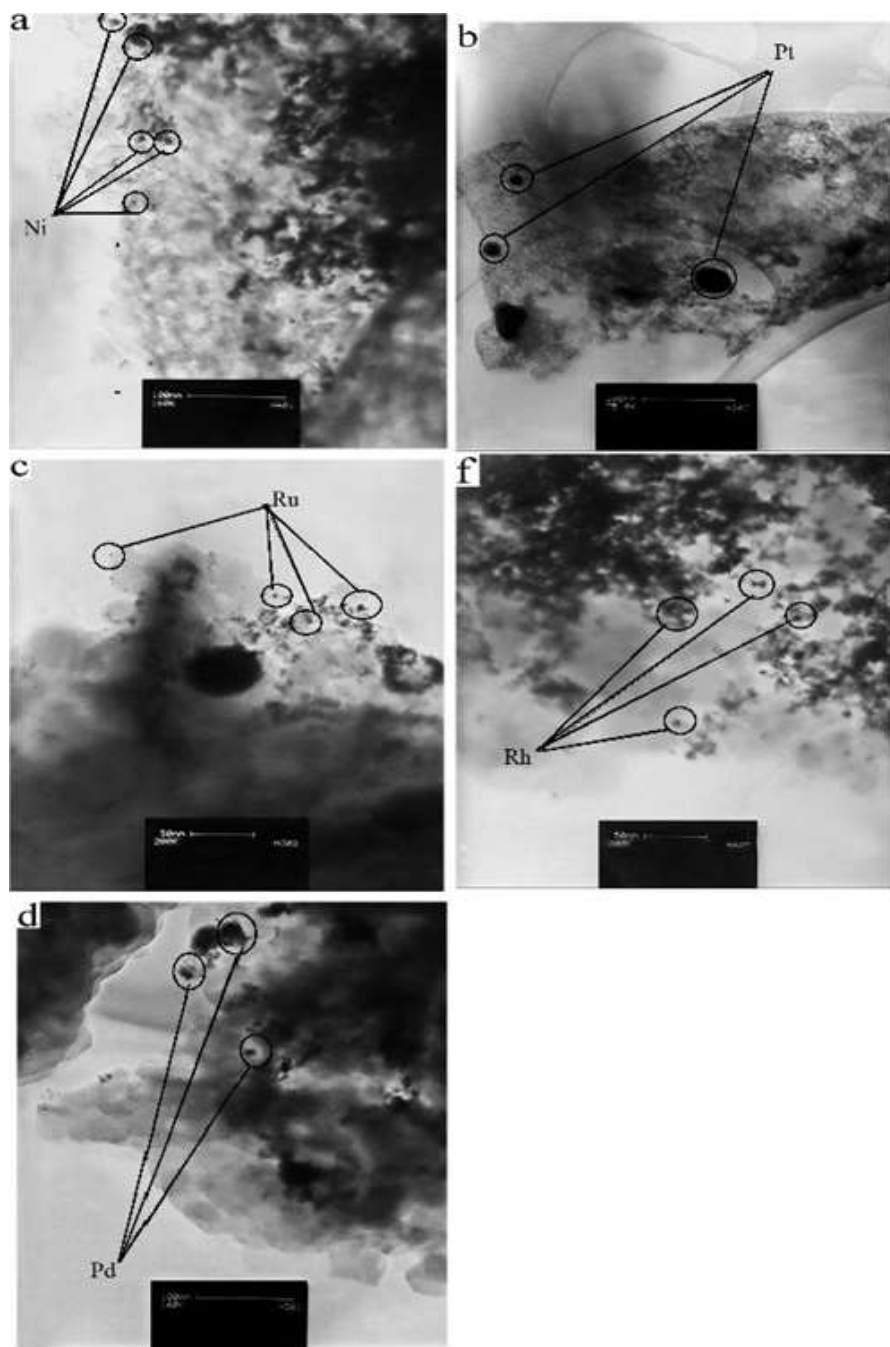


Fig. 3. TEM micrographs of the (a) Ni, (b) Pt, (c) Pd, (d) Ru and (e) Rh nanoparticles in the catalysts.

3.4. Interactive effect of process independent variables

The coded and encoded values of the test variables were used to optimize the variables experimental results of benzene hydrogenation percentage for each case are presented in Table 3. The efficiency of hydrogenation depends on individual effects and the results show significant variation for each combination. Multiple regression analysis of the experimental data was obtained from the following regression equation for the

hydrogenation of benzene: in which Y is the response variable or hydrogenation efficiency of benzene P , T , t and W are the coded values of the independent variables, pressure, temperature, reaction time and metal loading percentage, respectively.

$$Y_{Ni} = 55.8939 - 0.0228P - 0.0163T - 0.0176t + 2 \\ 7.7410W + 0.0007P^2 + 0.0001T^2 + 0.0001t^2 - \\ 0.3729W^2 + 0.0002PT + 0.0003Pt - 0.0023PW + \\ 0.0001Tt - 0.0012TW - 0.0007tW$$

The multiple regression coefficient (R^2) was estimated from the second-degree polynomial Eq. (2). The value of $R^2 = 0.911$, which is close to one, indicates that the

correlation is suitable for predicting the performance of the hydrogenation system and the predicted values were close to the experimental results (Fig. 4).

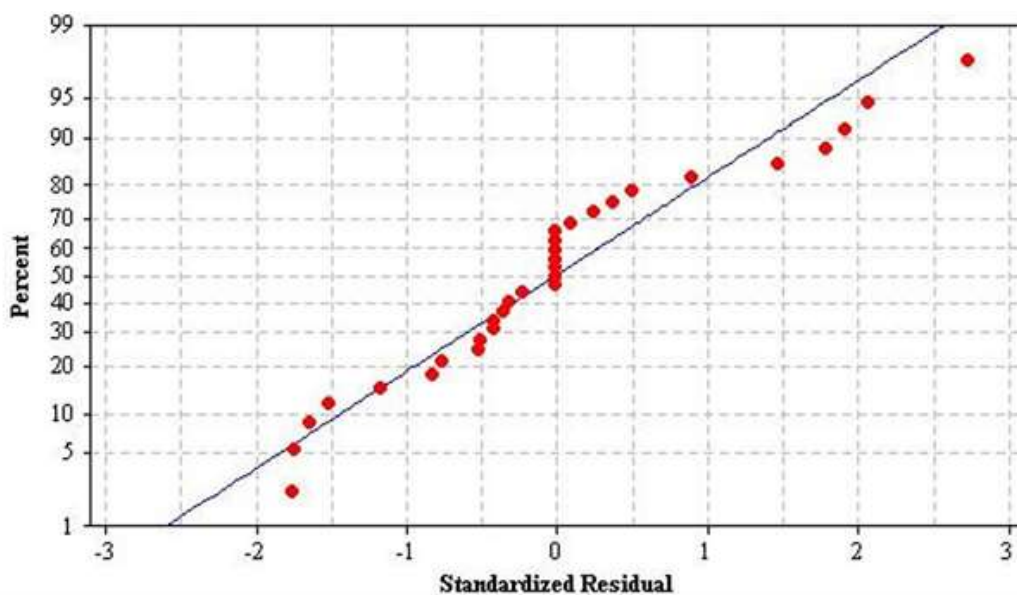


Fig. 4. Normal probability of the residuals (response efficiency %)

The optimum values of the test variables and the corresponding maximum percentage hydrogenation of benzene in gasoline for five catalysts were obtained in

uncoded units for the actual values, are given in Table 3.

Table 3. Optimum values of variables obtained from regression equations for the hydrogenation of benzene

Parameter	Optimum value				
	Rh	Ru	Pt	Pd	Ni
Pressure (atm)	50	50	50	50	50
Temperature (°C)	250	250	250	250	250
Time (min)	180	125	31.25	180	180
Loading (%)	10	10	10	9.64	9.56
Hydrogenation (%)	99.59	99.48	98.09	98.51	97.56

A maximum hydrogenation of 99.59 % was obtained using the rhodium catalyst under optimum conditions. This experimental values were compatible with the obtained values from the response surface methodology (RSM), confirming the fact that RSM that uses the statistical design of experiments is able to optimize the parameters effectively and to study the importance of the individual, cumulative and interactive effects of the test variables in hydrogenation. The results show that the activity of fullerene-based metal catalysts for the hydrogenation of benzene in gasoline is as follows: Rh

> Ru > Pd > Pt > Ni. However, this process is only based on efficiency and there is little difference between the yields. If we look at Table 3 we see that the reaction time of five catalysts is many different and the other parameters are the same values. These times are followed: 180, 125, 31.25, 180 and 180 min respectively. If we consider the reaction-time low following order of catalytic activity are Pt > Pd > Ru > Rh > Ni. Metals have different physical and chemical properties. So they have different catalytic activities. Since ruthenium catalysts were shown to be highly

active and selective for the hydrogenation of aromatic amines [63]. Whitman the usefulness of ruthenium as hydrogenation catalysts has been recognized by many other investigators in various hydrogenations [64]. Beeck was the first to note that rhodium is the most active of the transition metals for the hydrogenation of ethylene, as observed with evaporated metal films. Later, rhodium or rhodium-based catalysts were shown to be highly active for the hydrogenation of aromatic nucleus under very mild conditions [65].

As shown in TEM images (Fig. 3) Platinum and palladium nanoparticles have been in the pores of the surrounding space fullerenes. On the other hand, these images show that Pt nanoparticles are well dispersed and are evenly distributed on the fullerene support. According to the data of XRD and TEM size of the Pt nanoparticle are larger than the other catalysts. However, the larger the particle size distribution of the particles, causes it will increase the reaction rate of benzene hydrogenation.

The size of the Pd nanoparticle is less than other catalysts. However, as shown in XRD pattern, the crystallinity of this nanoparticle is less than other catalysts and the rate of hydrogenation is reduced compared with platinum. However, what is clearly seen in this study is that the use of fullerene as a base in the preparation of catalysts increased the efficiency of hydrogenation. It will definitely increase the active surface of the catalyst.

4. Conclusions

The current study involves the synthesis of various fullerene-based metal nanocatalysts (Ni, Pd, Pt, Ru and Rh) to use as a catalyst for the hydrogenation of benzene in gasoline. These catalysts have been characterized by different techniques and their activity for the hydrogenation of benzene in gasoline in a batch reactor has been tested. We have demonstrated the use of a full factorial central composite design by determining the optimum conditions leading to the maximum benzene hydrogenation to cyclohexane in gasoline. Using this experimental design and multiple regressions, the parameters, namely, pressure of hydrogen, temperature,

reaction time and loading were studied effectively and optimized with a lower number of experiments. The optimum values of variables obtained from regression equations for the hydrogenation of benzene show that the increase in these variables will increase the efficiency of hydrogenation. The optimized models predicted that the hydrogenation should be at a maximum level with the following conditions: for Rh catalysis the efficiency of Hydrogenation; 99.59 % (Rh loading ; 10%, reaction temperature; 250°C, reaction time; 180 min and hydrogen pressure; 50 atm), for Ru catalysis the efficiency of Hydrogenation; 99.48 % (Ru loading; 10%, reaction temperature; 250 °C, reaction time; 125 min and hydrogen pressure; 50 atm), for Pt catalysis the efficiency of Hydrogenation; 98.09 % (Pt loading; 10%, reaction temperature; 250 °C, reaction time; 31.25 min and hydrogen pressure; 50 atm), for Pd catalysis the efficiency of Hydrogenation; 98.51 % (Pd loading; 9.64%, reaction temperature; 250 °C, reaction time; 180 min and hydrogen pressure; 50 atm) and for Ni catalysis the efficiency of Hydrogenation; 97.56 % (Ni loading; 9.56%, reaction temperature; 250 °C, reaction time; 180 min and hydrogen pressure; 50 atm). The results show that the activity of fullerene-based metal catalysts for the hydrogenation of benzene in gasoline is as follows: Rh > Ru > Pd > Pt > Ni.

Acknowledgments

We thank Department of Chemistry of Bu-Ali Sina University and Ministry of Science and Research Institute of Petroleum Industry for supporting this study.

References

- [1] D.K. Verma, K. des Tombe, *AIHA J. Fairfax*, Va **63** (2002) 225.
- [2] International Agency for Research on Cancer, *IARC Monographs on the Evaluation of the Carcinogenic Risk of Chemicals to Humans*, 29 (1982) 93.
- [3] H. Krause, C. Dobler., *Catalysis letters*, **8** (1991) 23.

- [4] A. Pavlova, R. Ivanova, *Acta Chromatograph*, **13** (2003) 215.
- [5] L. Zoccolillo, M. Alessandrelli, M. Felli, *Chromatographia*, **54** (2001) 659.
- [6] A.P. Singh, S. Mukherji, A.K. Tewari, W.R. Kalsi, A.S. Sarpal, *Fuel*, **82** (2003) 23.
- [7] I. Uemasu, S. Kushiyama, *Fuel Process Technol*, **85** (2004) 1519.
- [8] A.A. Kinawy: *BMC Physiol*. 9 (2009) 1.
- [9] S. Nishimura, T. Itaya, M. Shiota: *Chem. Commun. (London)*, (1967) 422
- [10] Yi. Chen, D.L. Peng, D. Lin, X. Luo, *Nanotechnology* **18** (2007) 505.
- [11] Rules and Regulations, *Federal Register*, **72** (2007) 8487.
- [12] R.Z.C. van Meerten, J.W.E. Coenen, *J. Catal*, **37** (1975) 37.
- [13] R.Z.C. van Meerten, A.C.M. Verhaak, J.W.E. Coenen, *J. Catal*, **44** (1976) 217.
- [14] H.A. Franco, M.J. Phillips, *J. Catal*, **63** (1980) 346.
- [15] A. Jasik, R. Wojcieszak, S. Monteverdi, M. Ziolk, M.M. Bettahar, *J. Mol*, **242** (2005) 81.
- [16] A. Louloudi, J. Michalopoulos, N.H. Gangas, N. Papayannakos, *Appl. Catal*, **242** (2003) 41.
- [17] A. Louloudi, N. Papayannakos, *Appl. Catal. A*, **175** (1998) 21.
- [18] A. Louloudi, N. Papayannakos, *Appl. Catal. A*, **204** (2000) 167.
- [19] G. Marcelin, R.F. Vogel, H.E. Swift, *Appl. Catal*, **98** (1986) 64.
- [20] F. Mittendorfer, J. Hafner, *J. Phys.Chem*, **106** (2002) 13299.
- [21] R. Molina, G. Poncelet, *J. Catal*, **199** (2001) 162.
- [22] S. Toppinen, T.K. Rantakyla, T. Salmi, J. Aittamaa, *Ind. Eng. Chem. Res*, **35** (1996) 1824.
- [23] A. Lewandowska, S. Monteverdi, M.M. Bettahar, M. Ziolk, *J. Mol. A*, **3713** (2002) 1.
- [24] R. Wojcieszak, S. Monteverdi, M. Mercy, I. Nowak, M. Ziolk, M.M. Bettahar, *Appl. Catal, A*, **268** (2004) 241.
- [25] M.A. Ermakova, D.Yu. Ermakov, *Appl. Catal. A*, **245** (2003) 277.
- [26] A. Louloudi, N. Papayannakos, *Appl. Catal. A*, **204** (2000) 167.
- [27] R. Badilla-Ohlbaum, H.J. Neuburg, W.F. Graydon, M.J. Phillips, *J. Catal*, **47** (1977) 273.
- [28] M.I. Phillips, P.H. Emmett, *J. Catal*, **101** (1986) 268.
- [29] K.J. Yoon, M.A. Vannice, *J. Catal*, **82** (1983) 457.
- [30] J.M. Basset, G. Dalmai-Imelik, M. Primet, R. Mutin, *J. Catal*, **37** (1975) 22.
- [31] S.D. Lin, M.A. Vannice, *J. Catal*, **143** (1993) 539.
- [32] L.J. Simon, J.G. van Ommen, A. Jentys, J.A. Lercher, *Catal. Today*, **73** (2002) 105.
- [33] P. Chou, M.A. Vannice, *J. Catal*, **107** (1987) 129.
- [34] P. Chou, M.A. Vanice, *J. Catal*, **107** (1987) 140.
- [35] C. Milone, G. Neri, A. Donato, M.G. Musolino, *J. Catal*, **159** (1996) 253.
- [36] L. Ronchin, L. Toniolo, *Catal. Today*, **66** (2001) 363.
- [37] J.Q. Wang, P.J. Guo, S.R. Yan, M.H. Qiao, H.X. Li, K.N. Fan, *J. Mol. Catal. A Chem*, **222** (2004) 229.
- [38] J.W. da-Silva, A.J.G. Cobo, *Appl. Catal, A*, **252** (2003) 9.

- [39] S.W. Ho, J.M. Cruz, M. Houalla, D.M. Hercules, *J. Catal*, **135** (1992) 173.
- [40] J.M. Jablonski, D. Potocznapetru, J. Okal, L. Krajczyk, *React. Kinet. Catal. Lett*, **54** (1995) 15.
- [41] W.F. Taylor, *J. Catal*, **9** (1967) 99.
- [42] W.F. Taylor, H.K. Staffin, *J. Phys. Chem*, **71** (1967) 3314.
- [43] L.J. Simon, P.J. Kooyman, J.G. van Ommen, J.A. Lercher, *Appl. Catal. A*, **252** (2003) 283.
- [44] P. Tétényi, V. Galsan, *Appl. Catal. A*, **229** (2002) 181.
- [45] E. Zanjiri, M. Fazli, R. Seif Mohaddecy, M. Tyimouri, M. Aghababaei, *Journal of Applied Chemistry*, **3** (2013) 63.
- [46] T. Hino, T. Anzai, N. Kuramoto, *Tetrahedron Lett*, **47** (2006) 1429.
- [47] M.D. Tzirakis, J. Vakrosb, L. Loukatzikouc, V. Amargianitakisa, M. Orfanopoulousa, C. Kordulisb, A. Lycourghiotis, *J. Mol. Catal. A*, **316** (2010) 65.
- [48] E. Sulman, V. Matveeva, N. Semagina, I. Yanov, V. Bashilov, V. Sokolov. *J. Molecular Catal A, Chemical* **146** (1999) 257.
- [49] B. Coqa, J.M. Planeixb, V. Â. Brotons, *Appl. Catal. A*, **173** (1998) 175.
- [50] I. Spassova, M. Khristova, R. Nickolov, D. Mehandjiev. *J. Colloid Interface Sci*, **320** (2008) 186.
- [51] S.V. Pol, V.G. Pol, A. Frydman, G.N. Churilov, A. Gedanken, *J. Phys. Chem. B*, **109** (2005) 9495.
- [52] J.E. Fischer, P.A. Heiney, A.B. Smith III, *Acc. Chem. Res*, **25** (1992) 112.
- [53] L. Y. Chiang, L.Y. Wang, J. W. Swirczewski, S. Soled, S. Cameron, *J. Org. Chem*, **59** (1994) 3960.
- [54] J.P. Hare, T.J. Dennis, H.W. Kroto, R. Taylor, A.W. Allaf, S. Balm, et al, *J. Chem. Soc., Chem. Commun* (1991) 412.
- [55] J.D. Saxby, S.P. Chatfield, et al, *J. Phys. Chem.* **96** (1992) 17
- [56] JCPDS Powder Diffraction File, International Centre for Diffraction Data, Swarthmore.
- [57] S. Nath, D. Chakdar, G. Gope, *Nanotrends, A journal of nanotechnology and its application*, **2** (2007) 1.
- [58] S. Nath, D. Chakdar and G. Gope, D. Avasthi, *Journal of Nanoelectronics and Optoelectronics*, **3** (2008) 1.
- [59] R. Das, S.S. Nath, D. Chakdar, G. Gope, R. Bhattacharjee, *Journal of nanotechnology online*, (DOI : 10.2240/azojono0129).
- [60] M. Elisabeta., D. Barry, L. Robin, *Chemistry of Materials*, **22**(2010) 6555.
- [61] Yi. Chen, D.L. Peng, D. Lin, X. Luo, *Nanotechnology*, **18** (2007) 505.
- [62] L. C. Behr, J. E. Kirby, R. N. MacDonald, C. W. Todd, *J. Am. Chem. Soc.*, **68** (1946) 1296
- [63] G. M. Whitman, *U.S. Patent*. 2,606,925 (1952) [CA **1953**, 47, 3874i].
- [64] S. Nishimura, T. Itaya, M. Shiota.: *Chem. Commun.* (London), (1967), 422.
- [65] H. Krause, C. Dobler, *Catalysis Letters*, **8** (1991) 23.